Journal of Colloid and Interface Science 346 (2010) 17–22

Contents lists available at ScienceDirect

Journal of Colloid and Interface Science

www.elsevier.com/locate/jcis

Placement of alkanethiol-capped Au nanoparticles using organic solvents

Tae-Jin Yim [a], Hyeunseok Choi [a,c], Xiang Zhang [a,b,*]

[a] NSF Nanoscale Science and Engineering Center (NSEC), University of California, Berkeley, CA 94720, USA
[b] Materials Sciences Division, Lawrence Berkeley National Laboratory, Berkeley, CA 94720, USA
[c] Manufacturing System R&D Department, KITECH, 35-3, Hongcheon-ri, Ipjang-myeon, Cheonan-si, Chungnam 331-825, South Korea

ARTICLE INFO

Article history:
Received 5 October 2009
Accepted 21 February 2010
Available online 24 February 2010

Keywords:
Au nanoparticle
Nanoparticle placement
Organic solvent
Pinning

ABSTRACT

We report that alkanethiol-capped Au nanoparticles can be linearly placed by toluene with its physical properties as well as its wettability in the presence of the nanoparticles. It is visually confirmed that toluene can be pinned with the aid of the nanoparticles to transport the nanoparticles to pinned contacts and to form linear placements. Whether the nanoparticles in various solvents can be linearly placed or not is explained based on the results of evaporating the nanoparticle solutions and the physical properties of each solvent. Further studies on controlled placement of the nanoparticles by manipulating the physical properties of organic solvents or by selecting an organic solvent can lead to applications such as a waveguide and other optoelectronic devices.

1. Introduction

Exploring new ways to efficiently assemble nanoparticles into a placement is quite significant in regard to hopes for realizing nano-structured devices that can be applied to chemical [1] and biological [2] sensors, as well as optoelectronic devices such as data storage tools [3]. Thus far, researchers have developed assemblies of metal nanoparticles on block copolymers [4,5], and linear placements of nanoparticles [6–9]. For the linear placement of nanomaterials, solution-based placement is promising for easy and large-scale processes and for the dense and long one-dimensional placement of nanoparticles. Single walled carbon nanotubes (SWNTs) were placed by pinning surfactant-assisted aqueous dispersion of SWNTs on a polar self-assembled monolayer (SAM) [10]. Their pinning mechanism was supported by a previous simulation work [11]. The placement of nanoparticles through pinning is very prospective, not in terms of fabricating randomly filled nanoparticles on a SAM pattern, but as to placing single-nanoparticle lines in micro widths. If it is possible to reduce the number of nanoparticle layers to a single layer, such work could be utilized for applications such as for nanoparticle waveguides [12].

The focus of this work differs significantly from the placement of SWNTs [10] in some aspects. Instead of their aqueous medium which needs a surfactant to lower its contact angle, organic solvents can be used. The organic solvents can be evaporated without leaving debris behind. Nevertheless, the placement of nanoparticles through the pinning of organic solvents has not yet been elucidated. In this paper, we investigate whether various organic solvents can be utilized to place alkanethiol-capped Au nanoparticles on alternating polar/nonpolar SAMs (microcontact printed pattern). To this end, the linear placement mechanism will be associated with the pinning of solutions that are assisted by the concentration of the nanoparticles, width of the microcontact printed pattern, and the physical property of solvents.

As illustrated in Fig. 1, the linear placement of the nanoparticles in organic solvents on microcontact printed surfaces can result from the pinning effect of the nanoparticle solution. This pinning is the well-known "coffee stain" phenomenon [11,13–15]. The initial pinning of a solution containing the nanoparticles can be created by surface unevenness in the presence of the nanoparticles [13]. When a sessile droplet is pinned and the droplet evaporates, its contact angle decreases and the evaporation flux at the edge of the droplet is much higher than that at the pinned flow center [16]. Therefore, internal flows to the edge of the droplet keep the pinning line constant, while simultaneously transporting the nanoparticles to the pinned contact lines. The expectation that some organic solvents containing the nanoparticles could be pinned is supported by a previous report noting that nanoparticles were able to suppress dewetting in nanoparticle-filled polymer films [13,17]. The other factor affecting the linear placement of nanoparticles is the physical property of various organic solvents. Solvents used here have specific properties such as their contact angle, vapor pressure, and pinning property.

* Corresponding author. Address: NSF Nanoscale Science and Engineering Center (NSEC), 3112 Etcheverry Hall, University of California, Berkeley, CA 94720, USA.
E-mail address: xiang@berkeley.edu (X. Zhang).

0021-9797/$ - see front matter © 2010 Elsevier Inc. All rights reserved.
doi:10.1016/j.jcis.2010.02.050

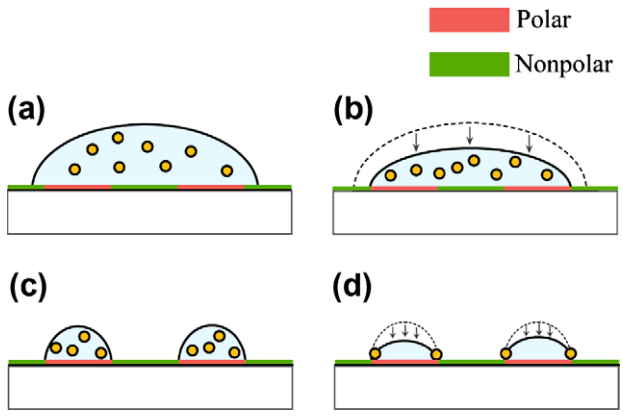

Fig. 1. Four steps in the formation of the nanoparticles placement on polar SAM, (a) a droplet placement of the nanoparticle solution, (b) solvent evaporation at macroscopic scale, (c) solvent pinning on polar SAM (no pinning in the absence of the nanoparticles), and (d) nanoparticles placement on the surface.

2. Materials and methods

2.1. Materials

Au nanoparticles were purchased from BBI international (Ted Pella, Redding, CA). SU8 (Negative tone photoresist) was purchased from Microchem (Newton, MA). The *Sylgard*® 184 silicon elastomer kit for Polydimethylsiloxane (PDMS) stamping was obtained from Dow Corning (Midland, MI). All other chemicals including 1-dodecanethiol, 11-mercapto-1-undecanol, and other solvents were purchased from Sigma–Aldrich (St. Louis, MO). All of the materials were used as they were originally received, without any further purification.

2.2. Fabrication for microcontact printing (fabrication of SU8 mold)

The substrate was cleaned and dried prior to applying a SU8 resist. The SU8 was used to make a mold for a PDMS stamp before coating the SU8 on a substrate (4 inch silicon (100) wafer, 500 μm). The silicon wafer was subjected to piranha etch/clean (H_2SO_4 and H_2O_2) for 10 min, and was then rinsed with DI water. To dry the surface, the substrate was baked at 200 °C for 5 min on a hot plate. After the cleaning process of the substrate, the SU8 was coated on the silicon wafer by a spin coater at 1000 rpm for 30 s. The coated resist thickness was ca. 4 μm, and was soft-baked to evaporate the solvent at 65 °C for one min and then at 95 °C for 3 min. The resist was exposed to UV (at 350 nm) on a mask aligner (MA6, Karl Suss America Inc., Waterbury, VT) in order to make the patterns. After the exposure, a post-bake was performed on a hot plate at 65 °C for one min and at 95 °C also for 1 min. SU8 developer was used to develop the exposed resist at room temperature for 1 min. The substrate was rinsed with isopropyl alcohol (IPA), and dried with nitrogen. The PDMS stamp was made using soft lithography with the fabricated SU8 mold. In order to remove its air bubble, a 10:1 (wt:wt) ratio of *Sylgard*® silicon elastomer to its curing agent was mixed and kept in a vacuum chamber for 30 min. This step was followed by pouring the PDMS on the SU8 mold. For curing, the PDMS and mold were kept in a vacuum oven at 85 °C for over 5 h. After the PDMS was completely cured, the PDMS stamp was slowly peeled off from the mold.

2.3. Functionalization of Au nanoparticles

All Au nanoparticles (60 nm in diameter, 7.8×10^{10} particles) in our experiment were functionalized with 5 mL of 2.5 mM 1-dodecanethiol in ethanol by overnight incubation. The 1-dodecanethiol-capped Au nanoparticles were then rinsed by redispersing them with sonication and by centrifuging to discard the supernatant. The nanoparticles were then finally ready to be dissolved in various organic solvents.

2.4. Microcontact printing

All of the sample surfaces had the same SAM on Au coated Si wafers treated with the microcontact printing (μ-CP) method [18]. To form a nonpolar SAM layer on the Au coated Si wafer surface, the fabricated PDMS stamp was inked with 4 mM 1-dodecanethiol in ethanol for 5 s, and μ-CP was carried out by slightly pressing the PDMS stamp. After μ-CP, the Au support was immersed in 12 mM 11-mercapto-1-undecanol in ethanol for 7 s so as to fill the 1-dodecanthiol-free spaces with the 11-mercapto-1-undecanol molecules. Next, the sample was removed from the solution, soaked in pure ethanol for about 10 s, and then dried under nitrogen gas. Finally, alternating polar/nonpolar SAMs on Au surface were obtained.

2.5. Formation of the linear nanoparticle placement

A small amount (5 μL) of the nanoparticles in each organic solvent (7.8×10^{10} particles/mL) was placed on a microcontact printed surface for observation.

2.6. Microscope observation

An upright microscope setup (Carl Zeiss MicroImaging Inc., Thornwood, NY) equipped with a camera was used to prove that the pinning of volatile organic solvents occurred.

2.7. Contact angle measurement

In order to approximate the contact angles on both polar and nonpolar SAM layered patterns, two surfaces for the polar and nonpolar SAMs were prepared by dipping Au coated wafers in ethanol solutions of 11-mercapto-1-undecanol and 1-dodecanethiol respectively, for 1 h. The contact angles of the solvents were measured three times with a contact angle measuring system (Kruss USA, Palo Alto, CA), and were averaged.

3. Results and discussion

Various organic solvents dissolving 1-dodecanethiol-capped Au nanoparticles (hereafter, the nanoparticles) were applied in order to induce the linear placement of the nanoparticles on microcontact printed surfaces. Our nanoparticles functionalized with 1-dodecanethiol are nonpolar and do not have strong interaction with each other unless a strong polar solvent like water is used. The surface for the linear placement was patterned with alternating layers of polar (11-mercapto-1-undecanoic acid, 4 μm in width) and nonpolar (1-dodecanethiol, 4 μm in width) thiol molecules, both of which are of similar length.

In Fig. 2, the placed nanoparticles using toluene are mainly positioned along the polar/nonpolar borderlines at 4 μm apart on the microcontact printed surface (alternating polar/nonpolar SAMs). As noted in the introduction, in order to explain the experimental result, it should be restated that the pinning of a solution is significant. When a drop of the nanoparticles in toluene at 15.6×10^{10} particles/mL was placed on the microcontact printed surface, the SAM layered surface resulted in filling with the nanoparticles. The reason is that a capillary force between the nanoparticles caused the filling of the nanoparticles [19,20]. However, less concentrated nanoparticles in toluene at 7.8×10^{10} particles/mL

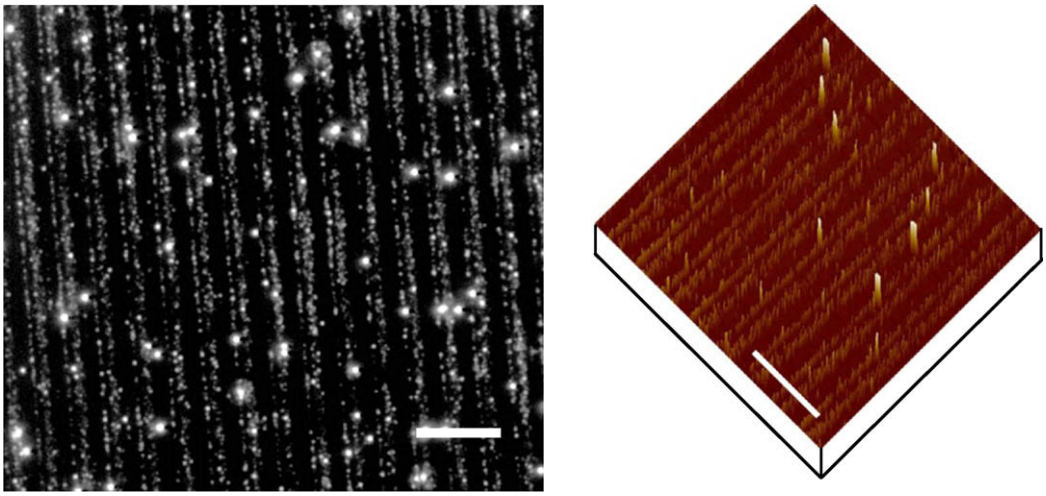

Fig. 2. Darkfield microscope and AFM images of nanoparticle placement through the pinned flow of toluene after placing the nanoparticles in toluene (at 7.8×10^{10} particles/mL) on the surface of alternating polar/nonpolar SAMs (scale bar: 20 μm).

produced a linear particle assembly with almost single lines at 4 μm apart. One of the reasons that the placement is not perfect can be existence of flows in the direction parallel to the pinned contact (polar/nonpolar borderline) as well as the flow to pinned contact. For better linear placement, a concentration of the nanoparticles that is too low (e.g., 15.6×10^9 particles/mL) should be avoided.

Because the nanoparticles in toluene at 15.6×10^9 particles/mL could not be pinned well, the nanoparticles were randomly positioned. However, when the nanoparticles were dissolved in toluene at 7.8×10^{10} particles/mL, the nanoparticles were well placed. These results can be explained in the following manner. In Fig. 3, the sequential placement mechanism of the nanoparticles in toluene at the intermediate concentration (7.8×10^{10} particles/mL) is depicted with microscope images illustrating that the toluene solution can be pinned in the presence of the nanoparticles. Once toluene was pinned to form cylindrical droplets on the polar SAM due to a lower contact angle than that on nonpolar SAM, it flowed internally toward the interface (pinned contact) between polar and nonpolar SAMs, and the nanoparticles in toluene were transported to the pinned contact lines [13].

The pinning of the nanoparticles in toluene solution appears to be limited. The area effect on the placement is also noteworthy. A gradient pattern (alternating nonpolar/gradient polar SAMs with 4 μm in width of nonpolar SAMs and 3–80 μm in width of polar SAMs) was used in order to see the formation of linear placements from cylindrical droplets on different width-scaled polar SAMs (Fig. 4). The linear placement was formed only in narrow pattern sizes (less than 5 μm). This result indicates that the nanoparticles in a cylindrical droplet with a smaller width are not only transported toward the pinned contact but also less adsorbed on polar SAM surface.

In order to investigate the effect of the other solvents on the placement of the nanoparticles, the same concentration of the nanoparticles as in Fig. 2 (toluene) was used. The placements with these solvents were found to be neither existent nor as good as those with toluene (Fig. 5). Interestingly, amongst the organic solvents used here, *only* toluene with the nanoparticles shows a pinning and linear placement of the nanoparticles at 7.8×10^{10} particles/mL (Table 1). Contrary to the pinning of toluene with the nanoparticles, pure toluene and other pure solvents were not pinned when placed on the microcontact printed surface. The pinning of solvents in the presence of the nanoparticles at 7.8×10^{10} particles/mL was not observed with *N*-hexane, dichloromethane, methanol, or *N*,*N*-dimethylformamide (DMF). The pinning properties of all solvents determining the placement of the nanoparticles can be explained by the contact angle and vapor pressure as follows.

As listed in Table 2, the contact angles of all organic solvents on polar SAM surfaces are lower than those on nonpolar SAM surfaces, which is in accordance with a previous report [21]. One requirement for pinning of a solution and transporting the nanoparticles is that the contact angle of a solvent droplet on polar SAM needs to be small [11,16]. The significance of a low contact angle can be explained as follows. The internal flow of a sessile droplet on a flat surface was derived by Hu and Larson [16], and the infinitely long cylindrical droplets on a flat surface were expressed in an analytical equation by Burganos and coworker (Eq. (1)) [11]

$$\langle V_x \rangle = -\frac{RJ_0}{\rho h_L(\sin\theta_c - \theta_c \cos\theta_c)}\left[\sin^{-1}(\bar{x}\sin\theta_c) - \theta_c \bar{x}\right] \quad (1)$$

where R is the radius of a cylindrical droplet, J_0 is the constant local evaporation flux across the surface of the liquid line, ρ is the liquid density, θ_c is the contact angle of the solution on polar SAM, and h_L is the height of the cylindrical liquid droplet at $\bar{x}$, dimensionless $\bar{x}$ is $\frac{x}{R}$. In this equation, vertically-averaged liquid velocity ($\langle V_x \rangle$, inside a kinetically controlled evaporating line for the pinned droplets lying on a substrate $(0 < \theta_c < \frac{\pi}{2})$) was expressed under the assumption of quasistatic flow [11]. It was also explained that a small contact angle is required for a higher vertically-averaged velocity. Therefore, it is reasoned that a low contact angle for an organic solvent can generate a high vertically-averaged velocity and consequently occurred internal flow can keep the pinning of the solution and transport the nanoparticles to complete the placement. In addition, contact angle contrast of nonpolar SAM to polar SAM is necessary for the pinning of the nanoparticle solution. As shown in Table 2, the contact angles were measured from droplets of organic solvents on polar and nonpolar SAMs, respectively.

Even though low contact angles for organic solvents on the polar SAM in contrast to those on the nonpolar SAM were satisfied, a certain level of vapor pressure is also necessary to obtain the pinned contacts and internal flow, and to transport the nanoparticles.

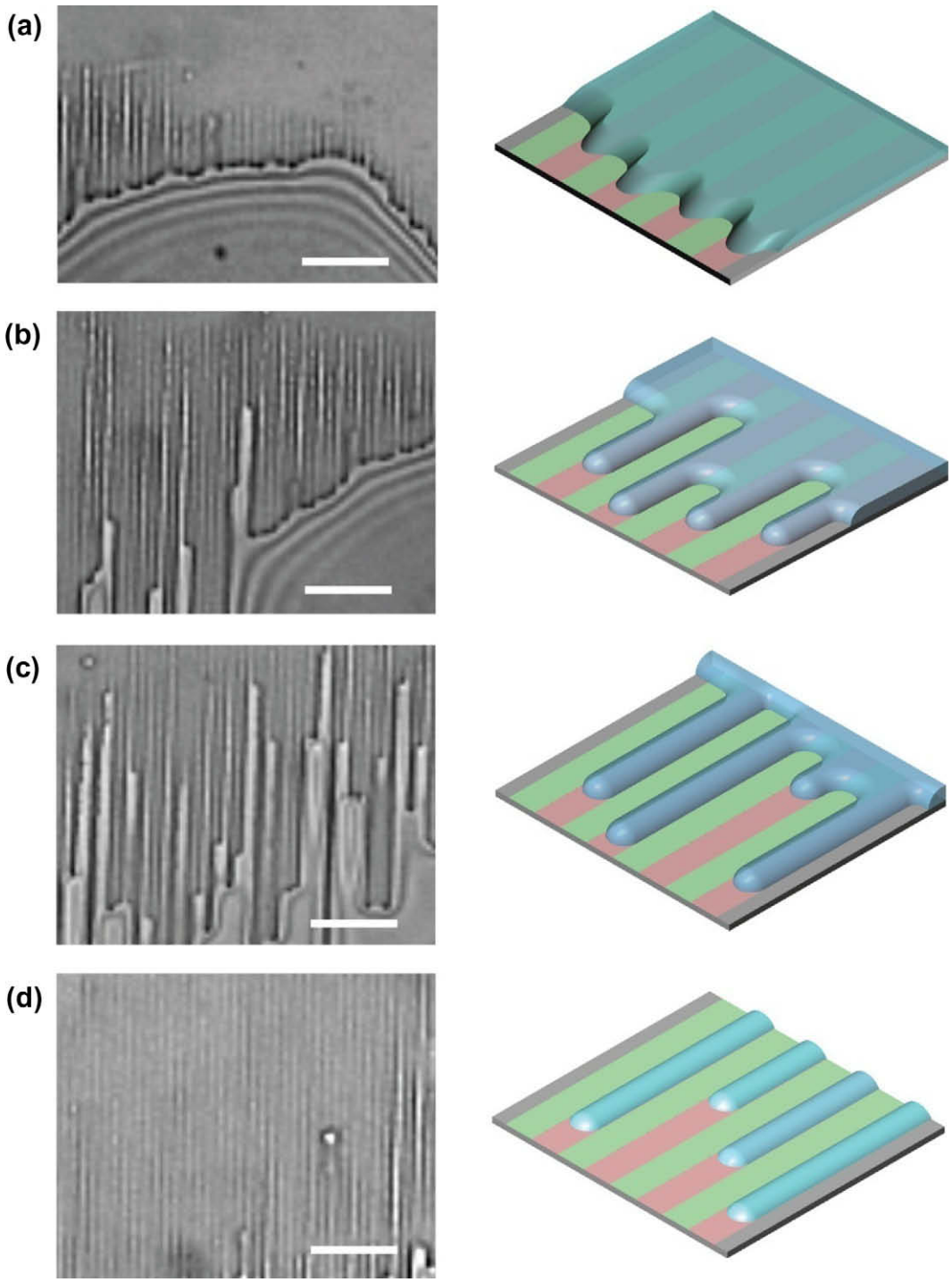

Fig. 3. Bright field microscope images of sequential nanoparticle placement through the pinned flow of toluene at (a) 7 s, (b) 7.8 s, (c) 8.3 s, and (d) 12 s after placing the nanoparticles in toluene on the surface of alternating polar/nonpolar SAMs (red: polar, green: nonpolar, and scale bar: 40 μm). (For interpretation of the references to color in this figure legend, the reader is referred to the web version of this article.)

The initial pinning property created by surface unevenness in the presence of nanoparticles can be enhanced while transporting nanoparticles with a certain level of vapor pressure as well as a low contact angle. It should be noted that citrate-stabilized Au nanoparticles were linearly placed by water in the presence of SDS as the 1-dodecanethiol-capped Au nanoparticles were linearly placed by toluene. To quantitatively compare the vapor pressures of pure organic solvents, the vertically-averaged liquid velocities of pure organic solvents were estimated based on the vertically-averaged liquid velocity of pure DMF (Table 2). It was used that the vertically-averaged liquid velocity is proportional to $[M]^{0.667} P^{vap}/T$. Water which has slightly lower vapor pressure than toluene supported the significance of the vapor pressure when it was used with the SDS to lower the contact angle. If the vapor pressure of a solvent is too high, droplets of the organic solvent containing the 1-dodecanethiol-capped nanoparticles cannot be well pinned since they collapse before transporting particles to the pinned contacts. Because the nanoparticles in highly volatile dichloromethane was not able to pin on the polar SAM (Fig. 5a), they formed various sizes of ring structures similar to such structures

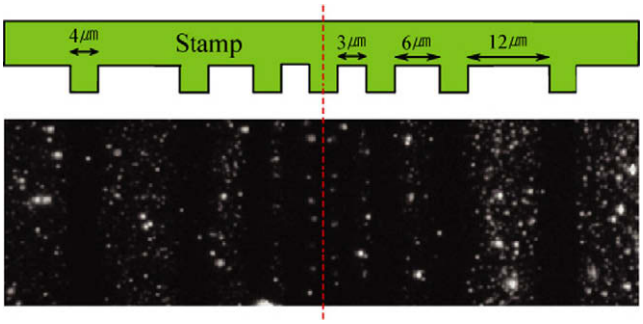

Fig. 4. Investigation of area effect by applying a gradient pattern (width of nonpolar SAM: 4 μm, and width of polar SAM: 3, 6, 12, 24 μm), where the nanoparticles in toluene at 7.8×10^{10} particles/mL was placed.

reported by Zubarev and coworker [22]. In Zubarev's report, nanorods assembled around water droplets that could condense from the air when highly volatile dichloromethane evaporated and cooled its flat surface below the dew point. Some similar ring shapes were also found in the nanoparticles in *N*-hexane which is also highly volatile, but the number of rings was much smaller than those observed in dichloromethane. In addition to the high vapor pressures of dichloromethane and *N*-hexane, incomplete placements were dominant due to their relatively low contact angle contrasts (Fig. 5a and b). In Fig. 5c, methanol's vapor pressure is relatively high, but the ring shape was not observed after drying the droplet of the nanoparticles. The entire area on the sample surface was kept wet at the beginning and the wetted line collapsed quickly instead of pinning the droplets microscopically on the polar SAM. On the other hand, a low vapor pressure for a solvent (low J_0 in (1)) cannot produce an internal flow rate high enough to carry the nanoparticles to the pinned contacts. This criterion can also be explained by Eq. (1). According to the vapor pressures listed in

Table 1
Effect of the nanoparticles on the pinning of organic solvents.

Solvent	Pinning (without the nanoparticles)	Pinning (with the nanoparticles at 7.8×10^{10} particles/mL)
N-Hexane	No	No
Toluene	**No**	**Yes**
Dichloromethane	No	No
Methanol	No	No
DMF	No	No

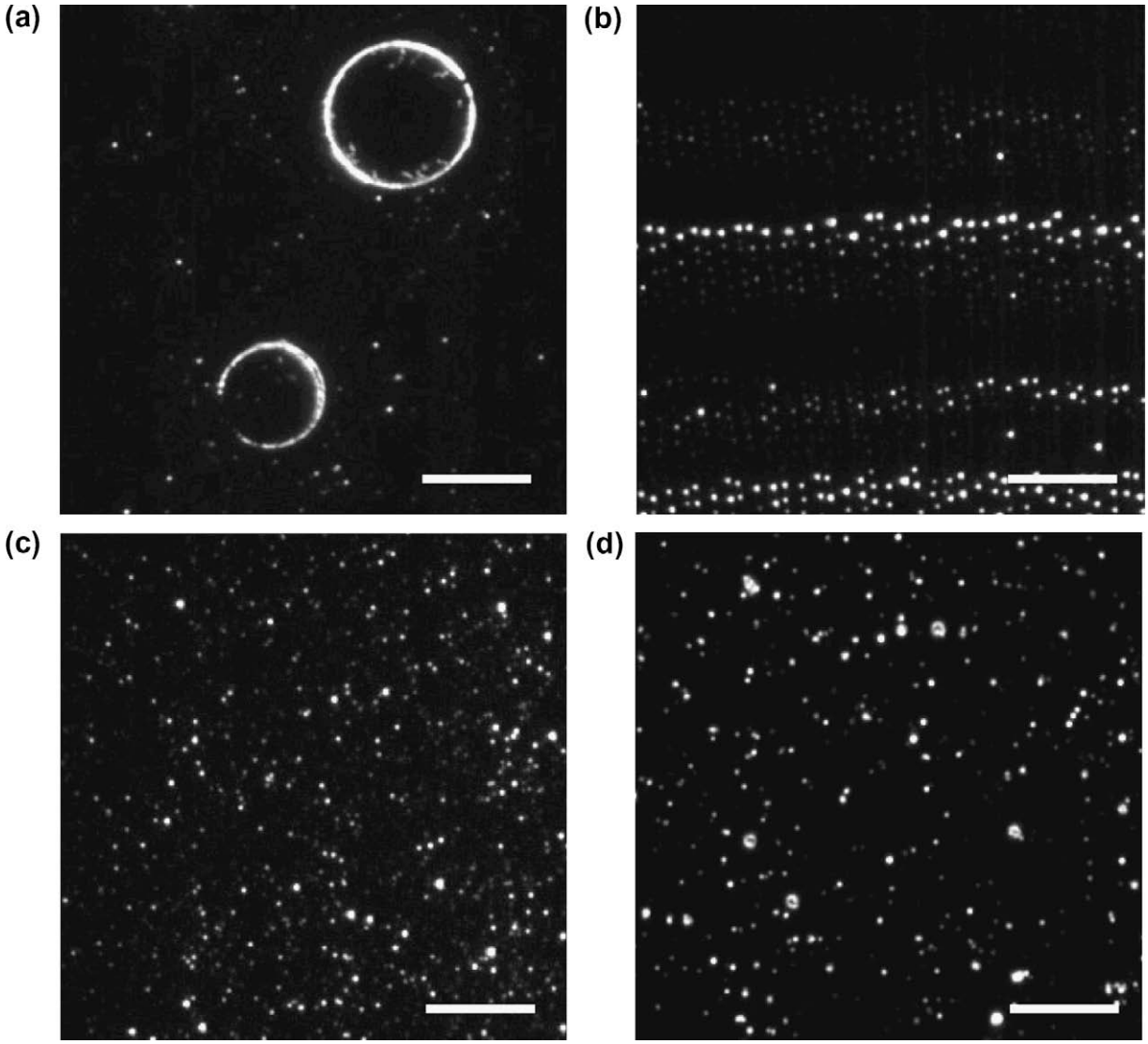

Fig. 5. Darkfield microscope images of dried nanoparticles after placing the nanoparticles in various solvents (at 7.8×10^{10} particles/mL) on the surface of alternating polar/nonpolar SAMs (scale bar: 20 μm). (a) dichloromethane, (b) *N*-hexane, (c) methanol, and (d) DMF with heating.

Table 2
Measured contact angles on each SAM and vapor pressures of pure solvents. For the estimated ratio of $\langle V_x \rangle$ to that of DMF, h_L was assumed to be same since θ_c (dichloromethane is 12.3 and all other solvents are 10 for the estimation) is very low on polar SAM.

Solvent	Measured contact angle		Vapor pressure at 25 °C (kPa) [23]	$\frac{\langle V_x \rangle}{\langle V_x \rangle_{DMF}}$ at $\bar{x} = 0.5$
	11-Mercapto-1-undecanoic acid (polar SAM)	1-Dodecanethiol (nonpolar SAM)		
N-Hexane	<10	9.8	20.2	71.6
Toluene	**<10**	**32.7**	**3.79**	**10.6**
Dichloromethane	12.3	18.6	58.2	101.8
Methanol	<10	36.8	16.9	30.4
Water	<10 with SDS		3.17	2.7
DMF	<10	61.6	0.439	1

Table 2, compared to other solvents, DMF has a low vapor pressure. Therefore, the placement of nanoparticles with DMF was not observed. However, heating to overcome the low vapor pressure of DMF was not relevant since the fluid was highly convective, consequently making its internal flow mechanism differ from volatile solvents, which evaporated over a free liquid surface (Fig. 5d). Likewise, when toluene was heated up to a temperature below its boiling point, droplet collapse was observed and no nanoparticle was linearly placed.

4. Conclusion

In summary, we studied an organic solvent based nanoparticle placement that resulted from the physical property of solvents and their wettability in the presence of nanoparticles. While toluene was found to be able to place alkanethiol-capped Au nanoparticles through pinning, the other organic solvents in this study were not able to do so. The linear placement mechanism was explained that the pinning of the nanoparticle solution at intermediate concentration and physical properties of toluene resulted in the placement of the nanoparticles in toluene on microcontact printed surfaces. Future efforts will extend our study to the optimization of thermodynamically controlled placement of nanomaterials, for example, by varying a vapor pressure or changing contact angles using different functional groups on surfaces. More studies on controlled placement with various factors are promising and may obtain either more impeccable or various-shaped positioning for applications such as chemical and biological sensing and nanoparticle waveguides in optoelectronic devices in the future.

Acknowledgments

We thank NIH Nanomedicine Development Center (Center for Cell Control, PN2 EY018228) and NSF Nano-scale Science and Engineering Center (NSEC, DMI-0327077) for support. H.C. acknowledges the financial support from the Korea Research Foundation Grant funded by the Korean Government (MOEHRD, Basic Research Promotion Fund) (KRF-2006-352-D00020).

References

[1] M. Suzuki, W. Maekita, Y. Wada, K. Nakajima, K. Kimura, T. Fukuoka, Y. Mori, Appl. Phys. Lett. 88 (20) (2006) 203121/1.
[2] K. Misiakos, S.E. Kakabakos, P.S. Petrou, H.H. Ruf, Anal. Chem. 76 (5) (2004) 1366.
[3] M. Todorovic, S. Schultz, J. Wong, A. Scherer, Appl. Phys. Lett. 74 (17) (1999) 2516.
[4] W.A. Lopes, H.M. Jaeger, Nature 414 (6865) (2001) 735.
[5] Q. Li, J. He, E. Glogowski, X. Li, J. Wang, T. Emrick, T.P. Russell, Adv. Mater. 20 (8) (2008) 1462.
[6] J. Huang, F. Kim, A.R. Tao, S. Connor, P. Yang, Nat. Mater. 4 (12) (2005) 896.
[7] Y. Cai, B.-M. Zhang Newby, J. Am. Chem. Soc. 130 (19) (2008) 6076.
[8] J. Bai, S. Huang, L. Wang, Y. Chen, Y. Huang, J. Mater. Chem. 19 (7) (2009) 921.
[9] R.R. Bhattacharjee, T.K. Mandal, J. Colloid Interface Sci. 307 (1) (2007) 288.
[10] R. Sharma, C.Y. Lee, J.H. Choi, K. Chen, M.S. Strano, Nano Lett. 7 (9) (2007) 2693.
[11] A.J. Petsi, V.N. Burganos, Phys. Rev. E 73 (4) (2006) 041201/1.
[12] S.A. Maier, P.G. Kik, H.A. Atwater, S. Meltzer, E. Harel, B.E. Koel, A.A.G. Requicha, Nat. Mater. 2 (4) (2003) 229.
[13] R.D. Deegan, O. Bakajin, T.F. Dupont, G. Huber, S.R. Nagel, T.A. Witten, Nature 389 (6653) (1997) 827.
[14] A.J. Petsi, V.N. Burganos, Phys. Rev. E 72 (4) (2005) 047301/1.
[15] T. Kajiya, D. Kaneko, M. Doi, Langmuir 24 (21) (2008) 12369.
[16] H. Hu, R.G. Larson, Langmuir 21 (9) (2005) 3963.
[17] K.A. Barnes, A. Karim, J.F. Douglas, A.I. Nakatani, H. Gruell, E.J. Amis, Macromolecules 33 (11) (2000) 4177.
[18] A. Kumar, H.A. Biebuyck, G.M. Whitesides, Langmuir 10 (5) (1994) 1498.
[19] N.D. Denkov, O.D. Velev, P.A. Kralchevsky, I.B. Ivanov, H. Yoshimura, K. Nagayama, Nature 361 (6407) (1993) 26.
[20] P.A. Kralchevsky, K. Nagayama, Langmuir 10 (1) (1994) 23.
[21] D. Janssen, R. De Palma, S. Verlaak, P. Heremans, W. Dehaen, Thin Solid Films 515 (4) (2006) 1433.
[22] B.P. Khanal, E.R. Zubarev, Angew. Chem., Int. Ed. 46 (13) (2007) 2195.
[23] D.R. Lide, CRC Handbook of Chemistry and Physics, electronic ed., CRC Press, Boca Raton, FL, 2001.